

INFORMATION TO USERS

This reproduction was made from a copy of a document sent to us for microfilming. While the most advanced technology has been used to photograph and reproduce this document, the quality of the reproduction is heavily dependent upon the quality of the material submitted.

The following explanation of techniques is provided to help clarify markings or notations which may appear on this reproduction.

1. The sign or "target" for pages apparently lacking from the document photographed is "Missing Page(s)". If it was possible to obtain the missing page(s) or section, they are spliced into the film along with adjacent pages. This may have necessitated cutting through an image and duplicating adjacent pages to assure complete continuity.
2. When an image on the film is obliterated with a round black mark, it is an indication of either blurred copy because of movement during exposure, duplicate copy, or copyrighted materials that should not have been filmed. For blurred pages, a good image of the page can be found in the adjacent frame. If copyrighted materials were deleted, a target note will appear listing the pages in the adjacent frame.
3. When a map, drawing or chart, etc., is part of the material being photographed, a definite method of "sectioning" the material has been followed. It is customary to begin filming at the upper left hand corner of a large sheet and to continue from left to right in equal sections with small overlaps. If necessary, sectioning is continued again—beginning below the first row and continuing on until complete.
4. For illustrations that cannot be satisfactorily reproduced by xerographic means, photographic prints can be purchased at additional cost and inserted into your xerographic copy. These prints are available upon request from the Dissertations Customer Services Department.
5. Some pages in any document may have indistinct print. In all cases the best available copy has been filmed.

**University
Microfilms
International**

300 N. Zeeb Road
Ann Arbor, MI 48106

1321379

CONNORS, CLIFFORD JAMES

THERMAL EXPANSION UNIFORMITY OF BOROSILICATE CROWN GLASSES
(TEMPAX AND E6)

THE UNIVERSITY OF ARIZONA

M.S. 1983

University
Microfilms
International 300 N. Zeeb Road, Ann Arbor, MI 48106

THERMAL EXPANSION UNIFORMITY
OF BOROSILICATE CROWN GLASSES (TEMPAX AND E6)

by
Clifford James Connors

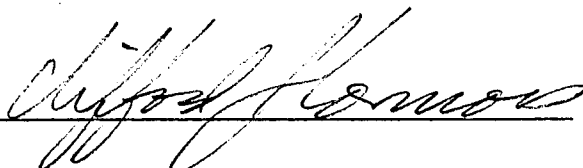
A Thesis Submitted to the Faculty of the
DEPARTMENT OF OPTICAL SCIENCES
In Partial Fulfillment of the Requirements
For the Degree of
MASTER OF SCIENCE
In the Graduate College
THE UNIVERSITY OF ARIZONA

1 9 8 3

STATEMENT BY AUTHOR

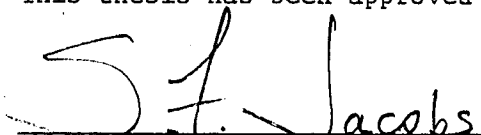
This thesis has been submitted in partial fulfillment of requirements for an advanced degree at The University of Arizona and is deposited in the University Library to be made available to borrowers under rules of the Library.

Brief quotations from this thesis are allowable without special permission, provided that accurate acknowledgment of source is made. Requests for permission for extended quotation from or reproduction of this manuscript in whole or in part may be granted by the head of the major department or the Dean of the Graduate College when in his judgment the proposed use of the material is in the interests of scholarship. In all other instances, however, permission must be obtained from the author.

SIGNED: 

APPROVAL BY THESIS DIRECTOR

This thesis has been approved on the date shown below:


S. F. Jacobs

Professor of Optical Sciences

7/26/83
Date

ACKNOWLEDGMENTS

I wish to thank Dr. Roger Angel, who conceived of and procured funding for this project, Dr. Stephen Jacobs for his continual guidance and support, and Mr. Richard Sumner for the expertly prepared samples.

TABLE OF CONTENTS

	Page
LIST OF ILLUSTRATIONS	iv
LIST OF TABLES	v
ABSTRACT	vi
1. INTRODUCTION	1
2. TECHNIQUES FOR MEASURING THERMAL EXPANSION UNIFORMITY . . .	4
3. EXPERIMENTAL METHOD	6
Theoretical Background	6
Apparatus	8
4. RESULTS AND ANALYSIS	12
5. CONCLUSIONS AND RECOMMENDATIONS FOR FURTHER RESEARCH . . .	19
APPENDIX 1. JUSTIFICATION OF APPROXIMATION	21
APPENDIX 2. THERMAL EXPANSION MEASUREMENT TECHNIQUE OF FURUARI	23
APPENDIX 3. PRACTICAL PROBLEMS ENCOUNTERED IN THE COURSE OF MEASUREMENT -- NOTES FOR FUTURE EXPERIMENTATION	24
SELECTED BIBLIOGRAPHY	28

LIST OF ILLUSTRATIONS

Figure		Page
1	Thermal Expansivity of Various Materials	3
2	Optical Arrangement to Illuminate Twin Fabry-Perot Etalons and Obtain Beat Frequency	9
3	Cutaway View of Sample Chamber	10
4	Sample Configuration for Confocal Resonator	11
5	Tempax Results	14
6	Compilation of Results	16
7	Method of Aligning End Mirrors on a Skewed Sample	25
8	Sample Data Set	27

LIST OF TABLES

Table		Page
1	Tempax Analysis	13
2	Remeasurements to Establish Repeatability	18

ABSTRACT

Thermal expansion uniformity is measured for Tempax and E6 Borosilicate Crown Glasses. Nine samples of Tempax are found to be homogeneous in thermal expansion within $2.7 \times 10^{-8}/^{\circ}\text{C}$ in the temperature range 30 to 45 $^{\circ}\text{C}$. The average experimental reproducibility is $.15 \times 10^{-8}/^{\circ}\text{C}$. The number of E6 samples is too small to support meaningful conclusions.

CHAPTER 1

INTRODUCTION

Thermal expansion uniformity is essential to the stability of the optical properties of large mirrors. It is the potential use of Borosilicate Crown Glass as the substrate for these mirrors which motivates this research.

Large mirror optical systems nearly always undergo temperature changes. Non-zero thermal expansivity of the mirror substrate will cause a shift in the focal plane with change in temperature. Therefore, the ideal substrate material will have low thermal expansivity. More importantly, the substrate material must have thermal expansion uniformity; inhomogeneities will cause image distortion which cannot be compensated.

Very low thermal expansivity materials (e.g., ULE, Cervit, etc.) are quite costly. Quartz is a compromise with $\alpha \approx .5 \times 10^{-6}/^{\circ}\text{C}$ at room temperature, but is still expensive. The thermal expansivity of Borosilicate Crown Glasses (BSC) is nearly an order of magnitude higher than that of quartz (see Figure 1 -- Pyrex is the BSC representative on this graph), but BSC is much less expensive. In addition, BSC can be conveniently cast into hollow-core mirror substrates which anneal very quickly. Thus, if they are sufficiently homogeneous, Borosilicate Crown Glasses are attractive candidates for large mirror substrate materials.

The BSC glasses chosen for this study are Tempax (manufactured by Schott), E6 (manufactured by Ohara), and "Palomar" (Type 7160 manufactured by Corning). Type 7160 is the material used in the construction of the 200 in. mirror of the giant telescope at Mt. Palomar, and in the 84 in. Kitt Peak telescope mirror. It is our understanding that this glass is no longer readily available; however, we included it in this study because so much is known about the performance of the telescope mirrors it was used to construct.

The uniformity is measured over the temperature range 30 to 45 °C.

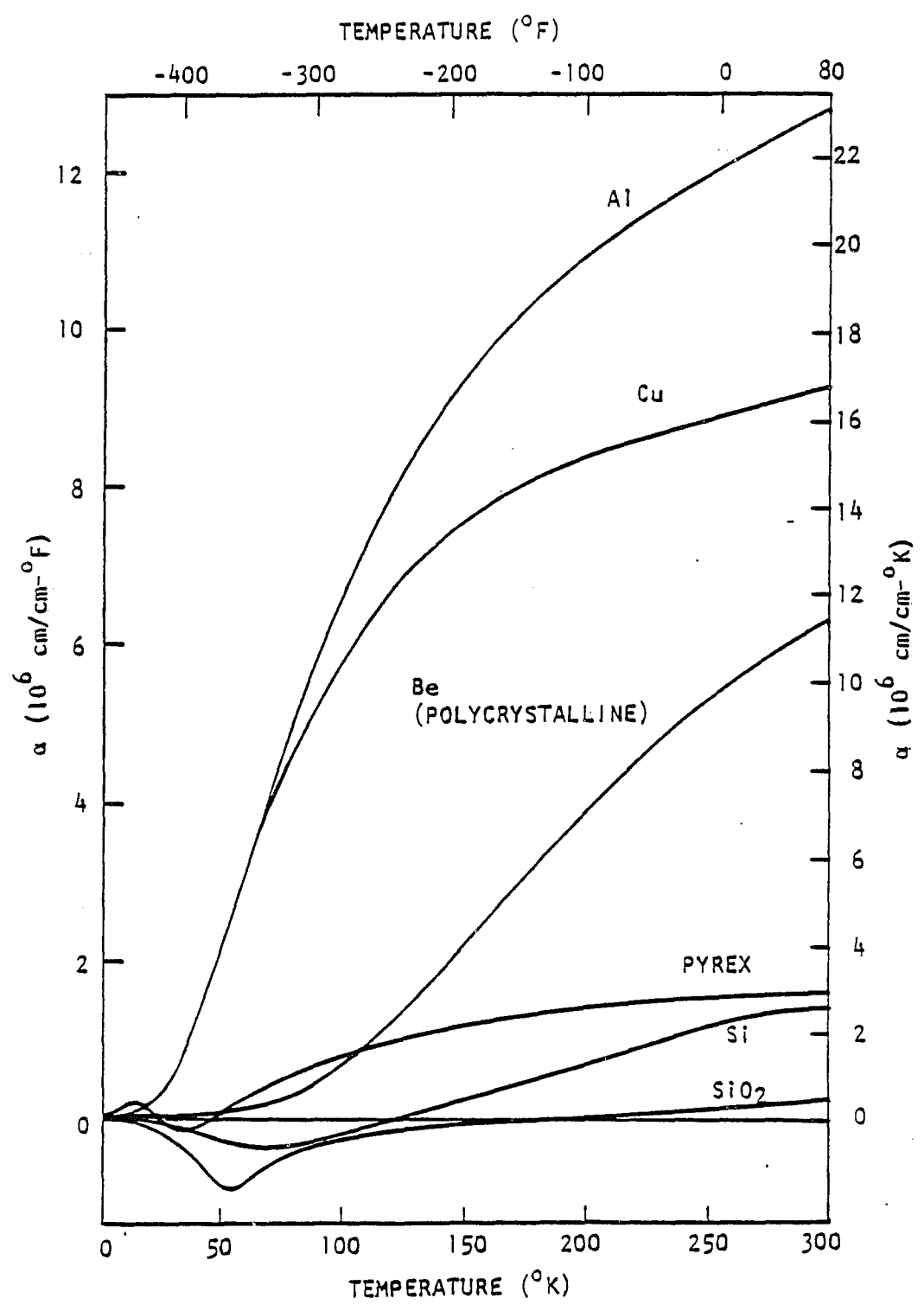


Figure 1. Thermal expansivity of various materials. (from Jacobs (1982))

CHAPTER 2

TECHNIQUES FOR MEASURING THERMAL EXPANSION UNIFORMITY

Modern materials are so homogeneous that existing methods for absolute thermal expansivity measurement have insufficient precision to detect inhomogeneities. Thus one cannot determine thermal expansivity differences by measuring two relatively large expansion coefficients and subtracting. Special techniques which measure thermal expansivity differences directly are therefore required. Two such differential methods are discussed below.

The first is the "sandwich seal" method of Hagy and Smith (1969). Here a sandwich of alternating materials (A-B-A or B-A-B) is sealed together at a temperature greater than the softening point of the glasses. After the sandwich is cooled, the residual stresses in the center piece are due to the difference in thermal expansion of the two glass types. The strain is determined photo-elastically based on the resulting birefringence of the glass sandwich. A problem with this method is that the determination of thermal expansion is very indirect, with calculations involving several stress parameters of the glasses and various assumptions. Thus other information about the glasses is prerequisite.

The other method of measuring thermal expansion uniformity is that used in this investigation. This interferometric technique was originally employed by Dean Shough (1981) in his PhD work at the University of Arizona. Fabry-Perot etalons are formed from the samples, and tunable lasers are locked to the samples and follow their length changes with changing temperature (as will be shown in Chapter 3). The difference frequency between the lasers (beat) is monitored. For two samples of identical thermal expansivity, the laser beat frequency remains constant as the sample temperature is varied. If the samples are not of identical thermal expansivity, the beat frequency will change as the sample temperature changes. This change in beat frequency with temperature variation can be readily related to the difference in thermal expansivity between the samples. The assets of this technique are the simplicity of interpretation and high accuracy. Drawbacks include costly sample preparation and restrictions on sample configuration (as will be evident from discussions next chapter).

CHAPTER 3

EXPERIMENTAL METHOD

Pairs of samples are placed together in a gradient-free temperature chamber (see Figure 3). When the chamber temperature is varied, the samples expand or contract and the optical cavities they form change length and therefore change resonance frequency. The tunable (slave) lasers follow these resonance changes, and the beat signal between the lasers is monitored (see Figure 2). The change in this beat frequency upon change in sample temperature is related to the difference in thermal expansivity between the samples as follows:

Theoretical Background

The beat frequency between two lasers of frequencies ν_1 and ν_2 is

$$f_{\text{beat}} = \nu_1 - \nu_2 \quad . \quad (1)$$

A thermal change ΔT results in the change

$$\Delta f_{\text{beat}} = \Delta \nu_1 - \Delta \nu_2 \quad . \quad (2)$$

The q^{th} order cavity resonance frequency is

$$\nu_i^q = \frac{qc}{2L_i n} \quad . \quad (3)$$

With index of refraction $n=1$, the differential change in frequency $\Delta \nu_i^q$ due to length change ΔL_i is

$$\Delta \nu_i^q = - \frac{qc \Delta L_i}{2L_i^2} = - \frac{\nu_i^q \Delta L_i}{L_i} \quad (4)$$

So

$$\Delta f_{\text{beat}} = \frac{\nu_2^q \Delta L_2}{L_2} - \frac{\nu_1^k \Delta L_1}{L_1} \quad (5)$$

From the definition of the thermal expansion coefficient,

$$\frac{\Delta L_i}{L_i} = \alpha_i \Delta T \quad ,$$

we have

$$\frac{\Delta f_{\text{beat}}}{\Delta T} = \nu_2^q \alpha_2 - \nu_1^k \alpha_1 \quad (7)$$

As shown in Appendix 1,

$$\nu_2^q \approx \nu_1^k \approx \nu_{\text{laser}} \quad (8)$$

with <.8% error in approximation. Thus equation (7) becomes

$$\frac{\Delta f_{\text{beat}}}{\Delta T} = \nu_{\text{laser}} (\alpha_2 - \alpha_1) \quad (9)$$

Rearranging further,

$$\alpha_2 - \alpha_1 = \frac{1}{\nu_{\text{laser}}} \left(\frac{\Delta f_{\text{beat}}}{\Delta T} \right) \quad (10)$$

Equation (10) is the deterministic equation: we seek the value of $(\alpha_2 - \alpha_1)$, and $\left(\frac{\Delta f_{\text{beat}}}{\Delta T} \right)$ is the measured quantity.

Apparatus

A top view of the optical table is shown in Figure 2. The He-Ne lasers are tunable by means of piezoelectric transducers attached to the glass laser tubes. The transducer strains the glass tube altering its length and therefore shifting the mode structure of the laser. The beams from the lasers are reflected up through the sample chamber (a cutaway view is provided in Figure 3). The samples are mounted in an evacuated thick-walled copper chamber to minimize thermal gradients. The photodetectors are located directly above the sample chamber, detecting the light transmitted through the Fabry-Perot cavities. The signals from these photodetectors are fed into lock-in amplifiers which maintain each slave laser frequency at its respective cavity resonance frequency. Portions of the beams are split off and interfered for beat signal monitoring. The beat signal from the photodetector is displayed on a panoramic spectrum analyzer (Tektronix Model 7613).

The sample configuration is shown in Figure 4. A hole (larger than the beam diameter) is bored through the cylindrical axis in order to make the refractive index of the optical cavity unity. Mirrors which make the cavity confocal are optically contacted to the ends of the samples. In addition, a small hole is drilled in the side of the sample to allow the cavity pressure to decrease to vacuum when the sample is in the evacuated chamber.

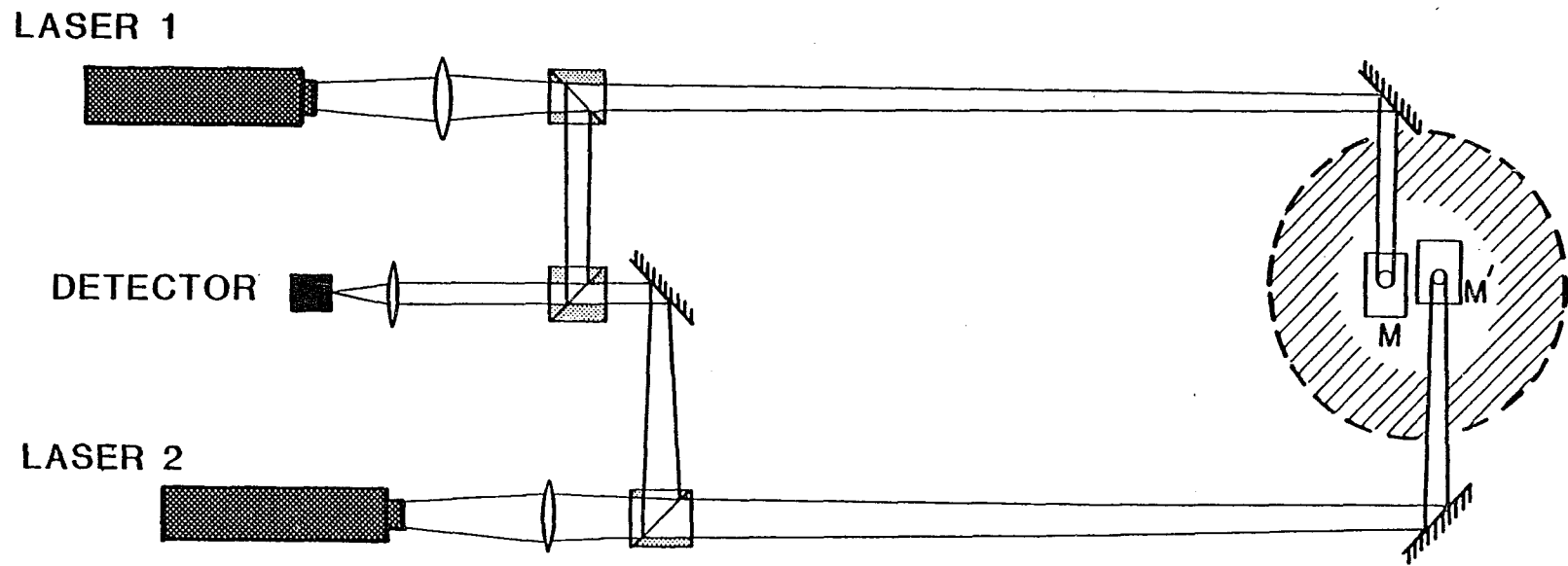


Figure 2. Optical arrangement to illuminate twin Fabry-Perot etalons and obtain beat frequency

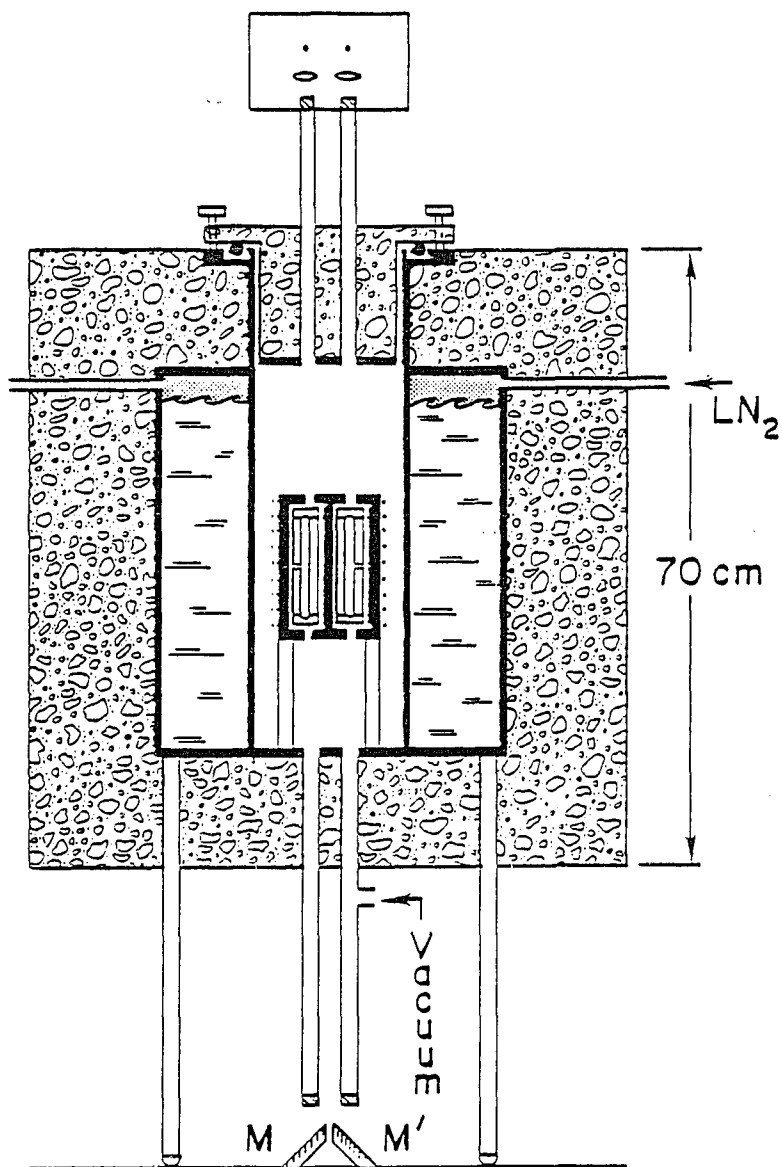
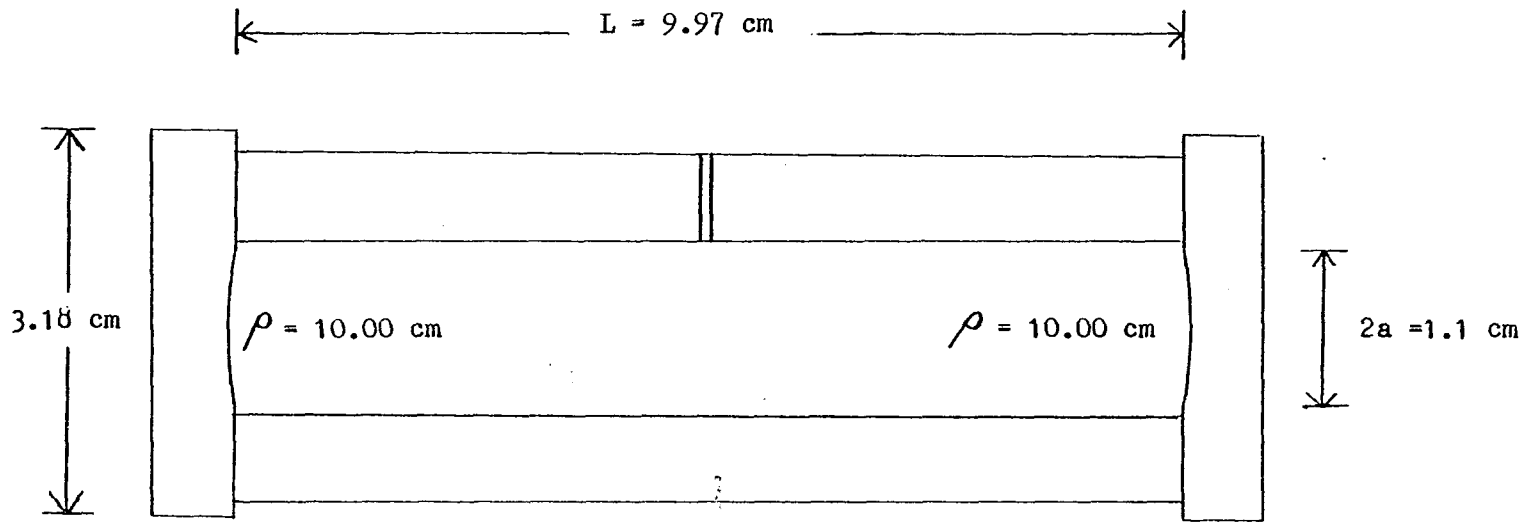


Figure 3. Cutaway view of sample chamber.



confocal, $\rho = 10.00 \text{ cm}$

$$L = \rho - 2s = 9.97 \text{ cm}$$

$$s \approx \frac{a^2}{2\rho} = .015 \text{ cm}$$

Figure 4. Sample configuration for confocal resonator.

CHAPTER 4

RESULTS AND ANALYSIS

A total of fourteen samples were tested: nine of Tempax, three of E6, and two of Corning "Palomar". The Corning samples were included to provide thermal expansion reference values in the neighborhood of those of Tempax and E6.

All Tempax samples were measured against Tempax Sample #17 as a reference (see Table 1); thus sample #17 has the value $\Delta\alpha = 0$ by definition. The E6 samples were measured against the sample "E6 Uncast". In addition, the Corning and several of the Tempax samples were also measured against "E6 Uncast" in order to plot all the results on one continuous graph (see Figure 6).

For an example of the format of one raw data set associated with a comparison of two samples, see Figure 8 in Appendix 3.

The results of the Tempax study are shown in Table 1 and Figure 5. The thermal expansion of the nine samples have a total spread of $2.7 \times 10^{-8}/^{\circ}\text{C}$ and a standard deviation of $.95 \times 10^{-8}/^{\circ}\text{C}$. Since the thermal expansivity of Tempax is approximately $320 \times 10^{-8}/^{\circ}\text{C}$, these nine samples exhibit the normalized values (total spread in α)/ $\alpha = .84\%$, and $\frac{\sigma_{\alpha}}{\alpha} = .30\%$.

Table 1. Tempax analysis.

Sample	$\Delta\alpha$ ($\times 10^{-8}/^{\circ}\text{C}$)	$\Delta\alpha - \overline{\Delta\alpha}$ ($\times 10^{-8}/^{\circ}\text{C}$)
Tempax #1	+0.05	+1.03
Tempax #13	0	+0.98
Tempax #17	0	+0.98
Tempax #4	-0.40	+0.58
Tempax #15	-0.83	+0.15
Tempax #8	-0.98	0
Tempax #11	-1.92	-0.94
Tempax #18	-2.09	-1.11
Tempax #7	-2.61	-1.63

Standard Deviation:

$$\sigma_{\alpha} = .95 \times 10^{-8}/^{\circ}\text{C}$$

Average Absolute Deviation:

$$\overline{|\Delta\alpha - \overline{\Delta\alpha}|} = .82 \times 10^{-8}/^{\circ}\text{C}$$

Total Spread:

$$= 2.66 \times 10^{-8}/^{\circ}\text{C}$$

(Δα measured with respect to Tempax #17)

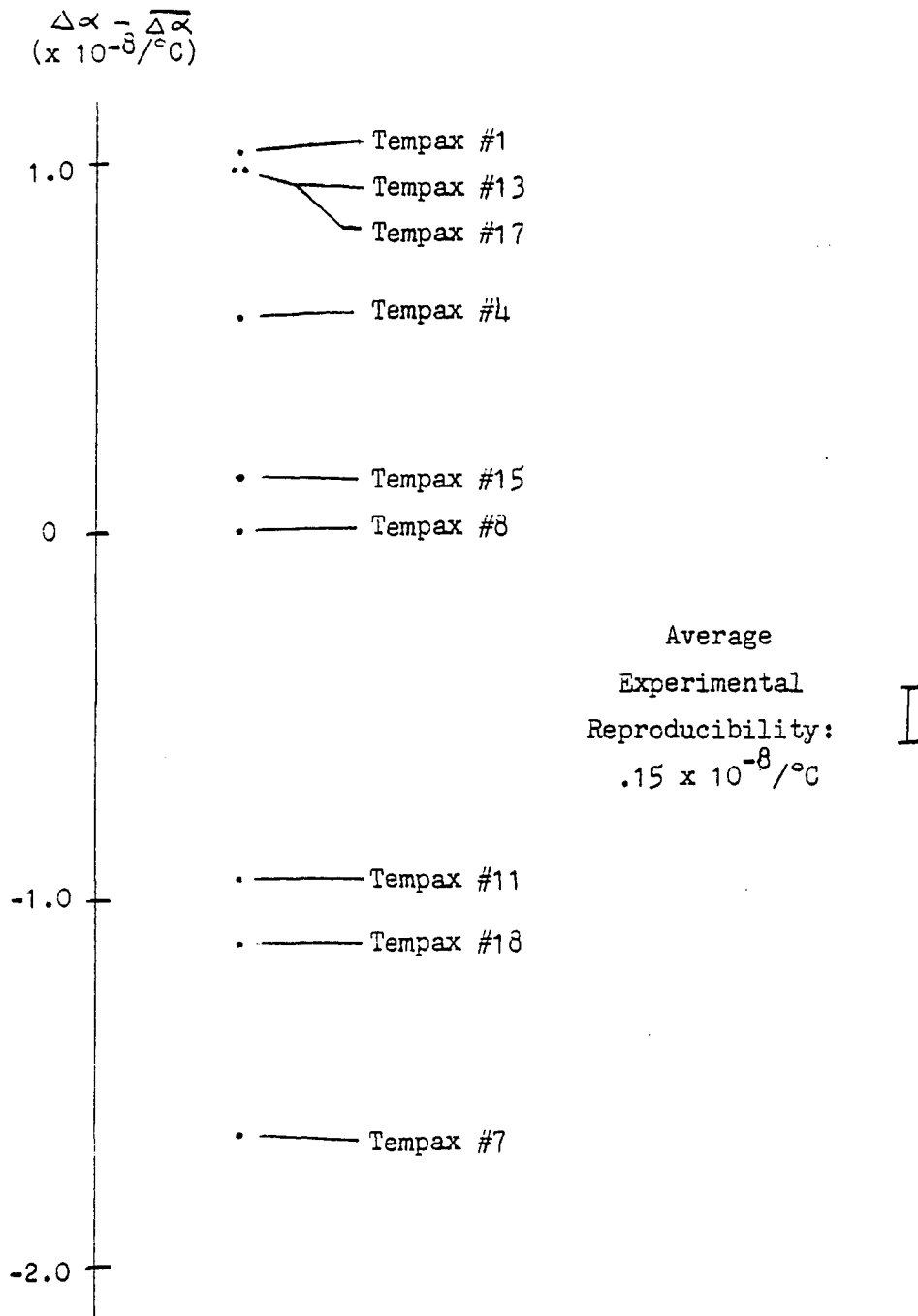


Figure 5. Tempax results.

The Tempax glass from which the samples were chosen was a two ton production in the form of 1/4 in. thick, 3 by 4 ft. sheets. Portions from various locations within the sheets, from various sheets across the production, were selected and cast to form the samples. It was of interest to determine whether the inhomogeneities of Tempax were due to systematic gradients across the production. However, the ordering of the samples in thermal expansivity could not be correlated to lot number, sheet number, or location within its sheet.

Figure 6 contains a graph with a broader scale, including the E6 and Corning glass results. The E6 material used was of two forms. We had in our possession only one chunk of E6 large enough to make a sample ("E6 Uncast"). The two other E6 samples (#20 and #21) were comprised of random bits and pieces of E6 which were cast into measurable samples. The two cast E6 samples exhibited the same thermal expansivity within the experimental accuracy, while the other E6 sample differed from them in thermal expansivity by $2.3 \times 10^{-8}/^{\circ}\text{C}$.

The two Corning samples consist of:

- 1) an uncast sample made from a souvenir ashtray.
This glass was furnished by California Institute of Technology and is purported to be identical to the glass in the 200 in. Mt. Palomar telescope mirror.
- 2) a cast sample of Corning Type 7160. This glass was furnished by Aden Meinel and is purported to be identical to the glass in the 84 in. Kitt Peak telescope mirror.

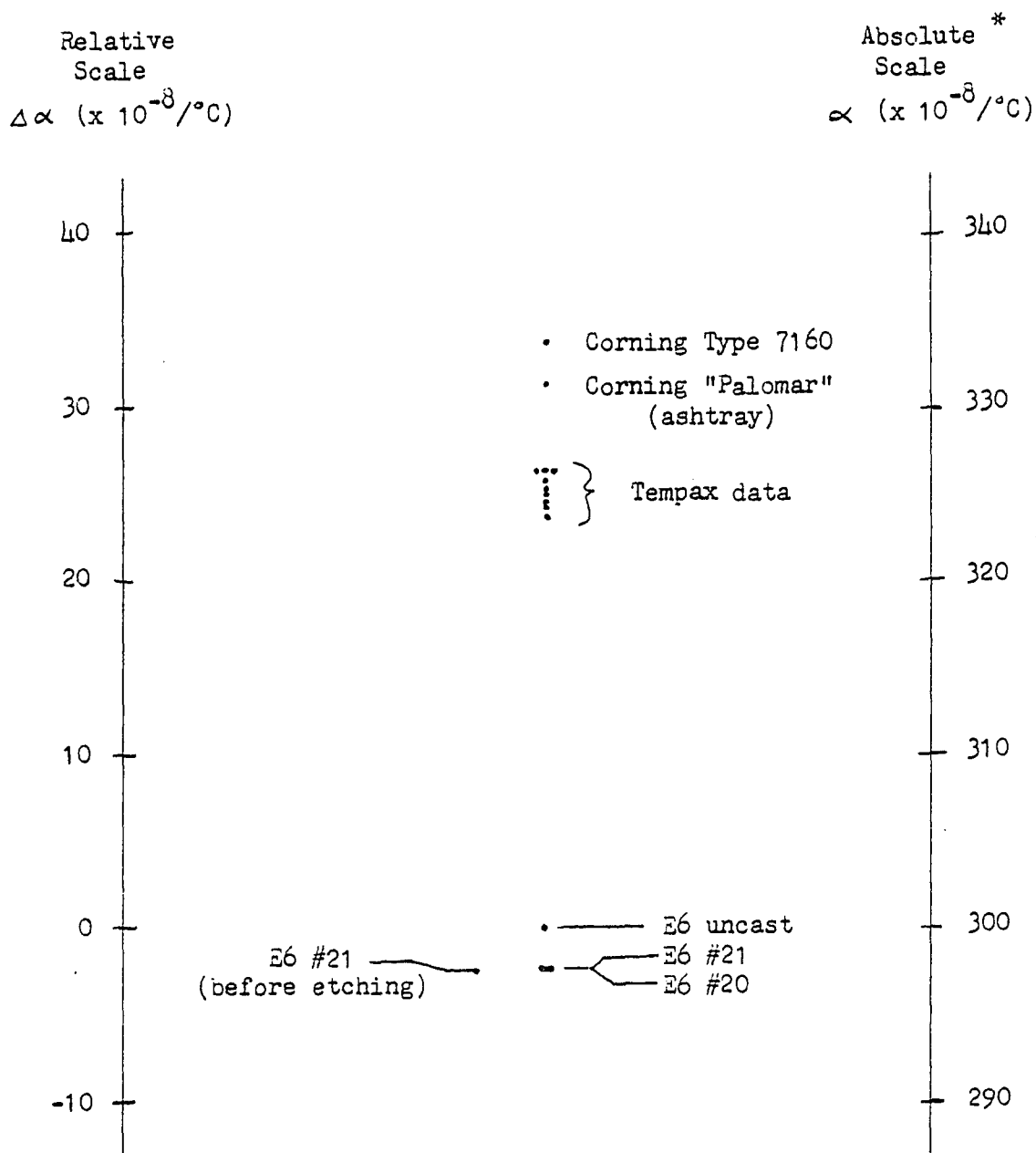


Figure 6. Compilation of results.

* These absolute expansivity values are approximate and based on personal communication with Dr. Roger Angel, University of Arizona.

During the casting process, a residue (from the mold) is deposited on the surface of the glass. Since the mirror substrates are cast, the effect this impure surface condition has on thermal expansion is of interest. Sample "E6 #21" was measured before and after this residue was etched from its surface. Before etching it measured $\Delta\alpha = 2.29 \times 10^{-8}/^{\circ}\text{C}$, and after etching it measured $\Delta\alpha = 2.27 \times 10^{-8}/^{\circ}\text{C}$. Since the difference is well within the experimental accuracy, it is concluded that for E6 the surface impurities associated with the casting process do not have a significant effect on thermal expansion.

In order to obtain a reliable estimate of the overall accuracy of the experiment, several samples were remeasured (see Table 2) and the differences from the original measurements analyzed. We remeasured two sample pairs (#15 vs. #17, and #7 vs. #17), and then measured several samples against sample #7, the lowest in thermal expansion of the group. The average difference between the original and the new measurements was $.15 \times 10^{-8}/^{\circ}\text{C}$, and this value is taken as the reproducibility. We believe the sources of error to be as follows:

- 1) thermal gradients. The sample chamber is constructed of thick-walled copper, and a minimum of 4 hours was allowed for each thermal equilibrium. Thus thermal gradients, though not measured, should be minimal.
- 2) human measurement. The beat frequencies were read directly from the spectrum analyzer. Error is estimated at ± 2 MHz.
- 3) curve fitting. The data always plotted into a very nearly straight line (see Figure 8, Appendix 3), and linear regression analysis was determined unnecessary. Estimated error in fitting curves is $\pm .05 \times 10^{-8}/^{\circ}\text{C}$.

Table 2. Remeasurements to establish repeatability.

Measured Samples	$\Delta\alpha (x 10^{-8}/^{\circ}\text{C})$	Expected Value of $\Delta\alpha (x 10^{-8}/^{\circ}\text{C})$ Based on Original Measurements	Discrepancy ($x 10^{-8}/^{\circ}\text{C}$)
#15 vs. #17	+0.96	+0.83	.13
#7 vs. #17	+2.49	+2.61	.12
#7 vs. #15	+1.75	+1.78	.03
#7 vs. #11	+0.88	+0.69	.19
#7 vs. #8	+0.78	+0.52	.26

Average Discrepancy: $.15 x 10^{-8}/^{\circ}\text{C}$

CHAPTER 5

CONCLUSIONS AND RECOMMENDATIONS FOR FURTHER RESEARCH

The nine Tempax samples had a total spread of $2.7 \times 10^{-8}/^{\circ}\text{C}$, corresponding to a normalized value (total spread in α)/ $\alpha = .84\%$. This is comparable to the Heraeus-Amersil Fused Quartz (T08E) results of Shough (1981), who found for eleven samples from three melts a total spread of $.5 \times 10^{-8}/^{\circ}\text{C}$, corresponding to the normalized value (total spread in α)/ $\alpha = 1.0\%$.

The two E6 samples which were comprised of arbitrarily collected scraps exhibited the same thermal expansivity within the experimental accuracy. However, this may well have been due to a fortunate averaging of widely diverse elements. The third E6 sample (E6 Uncast) had a thermal expansivity significantly different from the two cast samples ($\Delta\alpha = 2.3 \times 10^{-8}/^{\circ}\text{C}$). Because of the small number of similarly prepared samples investigated, we hesitate to draw any conclusions regarding E6.

It is still of interest to learn whether the uniformity of E6 surpasses that of Tempax, and further E6 measurements are being planned for the very near future. It should be noted that E6 glass has been tested for thermal expansion homogeneity by Furuari (1982) who found, for 11 samples from 5 meltings, that the homogeneity was $4 \times 10^{-8}/^{\circ}\text{C}$ (compared with $2.7 \times 10^{-8}/^{\circ}\text{C}$ for nine samples of Tempax).

However, Furuari employed an absolute method (see Appendix 2) with less precision than in the Tempax results discussed above. Thus a definitive series of high accuracy measurements of E_6 is still motivated.

APPENDIX 1

JUSTIFICATION OF APPROXIMATION

We begin with equation (7):

$$\frac{\Delta f_{\text{beat}}}{\Delta T} = \nu_2^q \alpha_2 - \nu_1^k \alpha_1 \quad . \quad (7)$$

Let us define ν_{laser} as the center of the He-Ne laser transition.

Then we re-write equation (7) as follows:

$$\frac{\Delta f_{\text{beat}}}{\Delta T} = \left[\nu_{\text{laser}} - (\nu_{\text{laser}} - \nu_2^q) \right] \alpha_2 - \left[\nu_{\text{laser}} - (\nu_{\text{laser}} - \nu_1^k) \right] \alpha_1 \quad . \quad (11)$$

Combining terms,

$$\frac{\Delta f_{\text{beat}}}{\Delta T} = \nu_{\text{laser}} (\alpha_2 - \alpha_1) + (\nu_2^q - \nu_{\text{laser}}) \alpha_2 - (\nu_1^k - \nu_{\text{laser}}) \alpha_1 \quad . \quad (12)$$

Now we compare the magnitudes of the terms to justify the approximation of dropping the last two terms. For two samples homogeneous to within the accuracy of this experiment ($.15 \times 10^{-8}/^\circ\text{C}$):

$$\left(\frac{\alpha_2 - \alpha_1}{\alpha_1} \right)_{\text{min}} \approx \left(\frac{\alpha_2 - \alpha_1}{\alpha_2} \right)_{\text{min}} \approx \frac{.15 \times 10^{-8}}{300 \times 10^{-8}} = 5 \times 10^{-4} \quad . \quad (13)$$

The term $(\nu_i - \nu_{\text{laser}})$ is bounded in magnitude by the halfwidth of the Doppler broadened laser transition (from Yariv):

$$\Delta \nu_d \approx 1 \times 10^9 \text{ Hz} \quad . \quad (14)$$

So,

$$\left(\frac{\nu_2^q - \nu_{\text{laser}}}{\nu_{\text{laser}}} \right)_{\text{max}} = \left(\frac{\nu_1^k - \nu_{\text{laser}}}{\nu_{\text{laser}}} \right)_{\text{max}} \approx \frac{10^9}{5 \times 10^{14}} = 2 \times 10^{-6} \quad . \quad (15)$$

Hence the ratio of the minimum value of term #1 (on the right side of equation (12)) to the maximum value of term #2 or term #3 is:

$$\frac{\nu \cdot \Delta\alpha_{\min}}{\alpha \cdot \Delta\nu_{\max}} = \frac{\nu}{\Delta\nu_{\max}} \cdot \frac{\Delta\alpha_{\min}}{\alpha} = \frac{5 \times 10^{-4}}{2 \times 10^{-6}} = 250 \quad . \quad (16)$$

Thus the first term is larger than either of the others by a factor of 250 in the worst case. For a typical value of $\Delta\alpha = .5 \times 10^{-8}/^{\circ}\text{C}$, this factor rises to 800. Thus the approximation is quite safe:

$$\frac{|\text{term \#2}| + |\text{term \#3}|}{|\text{term \#1}|} \leq .8\% \quad . \quad (17)$$

APPENDIX 2

THERMAL EXPANSION MEASUREMENT TECHNIQUE OF FURUARI

This is a Fizeau interferometric method (Furuari (1982)) for measuring absolute thermal expansion, and then determining homogeneity by comparing the thermal expansion results for the various samples. Furuari states that his accuracy is $\pm 5 \times 10^{-8} / ^\circ\text{C}$. The technique involves sandwiching the sample between a flat mirror and a wedged plate. The changes in sample thickness are determined by an automated fringe counting arrangement. This method is attractive in that the thermal expansion results are arrived at very simply and directly, however, the method would be more accurate for homogeneity determination if it compared samples differentially. Perhaps an arrangement with two samples separated by a known lateral distance and sandwiched between two flat plates would be an improvement. Then the fringe separation would be the variable of interest.

APPENDIX 3

PRACTICAL PROBLEMS ENCOUNTERED IN THE COURSE OF MEASUREMENT -- NOTES FOR FUTURE EXPERIMENTATION

This appendix is directed to the reader interested in the practical details of making measurements on this apparatus, and to the successors of the author who will be undertaking similar measurements in the future.

Sample Preparation

When contacting the disc shaped end mirrors onto the samples, much of the difficulty in alignment of the samples can be avoided by making sure that the discs share the same cylindrical axis. Often the samples do not form perfect cylinders (are skewed), but their end faces are always parallel. Thus when contacting the second end mirror, the sample should be rotated and the position of the second end mirror should be chosen such that the mirrors share the same axis of rotation (do not wobble with respect to each other). This is facilitated by rotating the sample with the bottom (contacted) mirror tangent to a flat vertical surface (see Figure 7), and positioning the top mirror such that it is also tangent to the surface. This eliminates off-axis mode difficulties and reduces the magnitudes of the adjustments involved in aligning the beams up through the samples.

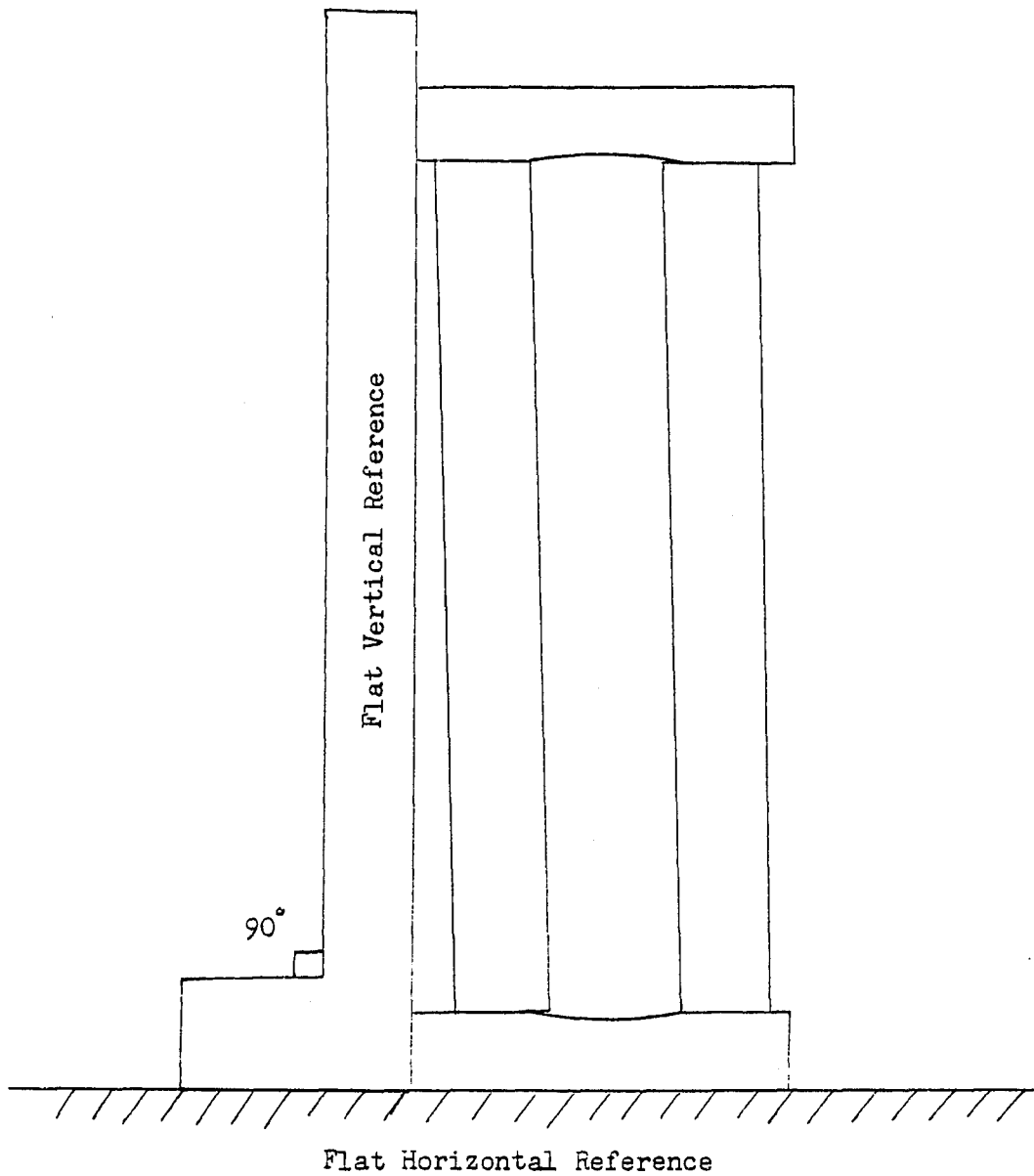


Figure 7. Method of aligning end mirrors on a skewed sample.

Alignment

The simplest method for aligning the samples is to observe what the lock-in amplifier sees. This is facilitated by sweeping the laser frequency by applying the high-voltage output of a ramp generator to the piezoelectric transducer on the laser tube. Then view the signal from the photodetector on an oscilloscope (triggered by the ramp generator). Now align the beam up through the sample chamber so as to maximize the magnitude and sharpness of the resonance peak (Fabry-Perot etalon response).

Measurement

The direction (sign) of the beat signal must be established in some arbitrary but consistent way. The method used by the author was to break the lock on the "A" sample by manually tuning the "A" laser with a clockwise rotation of the manual tuner. The direction of the resulting motion of the beat signal indicates its sign.

It is important to be certain that the panoramic spectrum analyzer is accurately calibrated. This should be checked from time to time.

In order to save time reaching equilibrium, it is best to take data with increasing temperature. This is because the heating coil adds heat in a relatively uniform fashion (through all the curved surfaces of the cylinder), but externally aided cooling occurs asymmetrically (i.e., liquid nitrogen coolant poured into the bottom of the chamber at first cools only the base plate).

A sample data set is provided in Figure 8.

Tempax #11 vs. Tempax #17

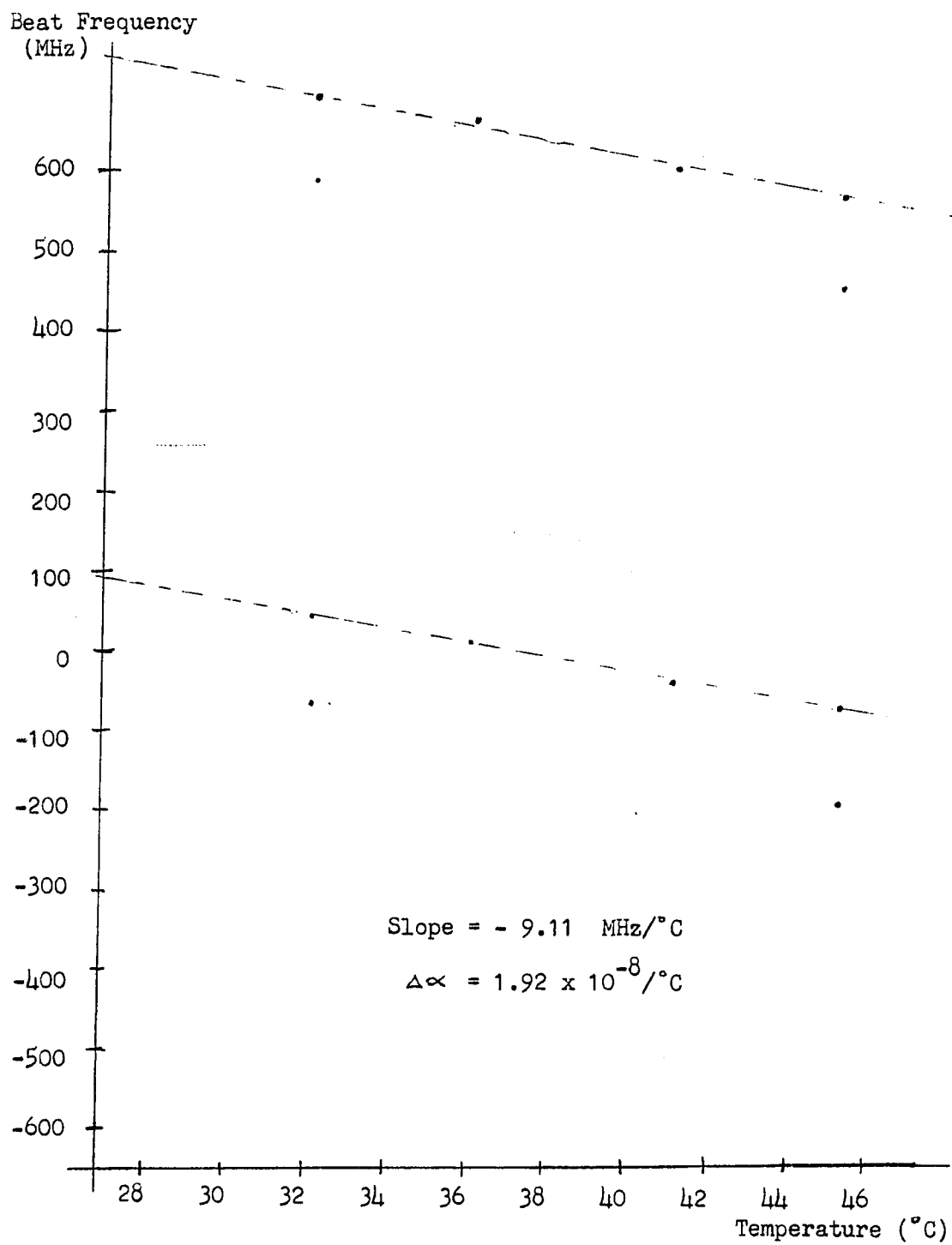


Figure 8. Sample data set.

SELECTED BIBLIOGRAPHY

- Furuari, Y., et al. Research on New Type of Mirror for Extra Large Telescope. Tokyo University, April 1982.
- Hagy, H. E. High Precision Photoelastic and Ultrasonic Techniques for Determining Absolute and Differential Thermal Expansion of Titania-Silica Glasses. Applied Optics, Vol. 12, pp. 1440-1446, July 1973.
- Hagy, H. E., and A. F. Smith. Sandwich Seal in the Development and Control of Sealing Glasses. J. Canadian Ceramic Society, Vol. 38, p. 63, 1969.
- Jacobs, S. F. "Dimensional Stability" in McGraw-Hill Yearbook of Science and Technology 1982. McGraw-Hill, New York, 1982.
- Shough, Dean. Creation of a New Facility for Measuring Thermal Expansion and Studies on the Homogeneity of Heraeus-Amersil Fused Silica. Ph.D. Dissertation, University of Arizona, Tucson, Arizona, 1981.
- Volf, M. B. Technical Glasses. Isaac Pitman and Sons, London, 1961.
- Yariv, Amonon. Introduction to Optical Electronics. Second Edition. Holt, Rinehart, and Winston, New York, 1976.